Raman analysis of DLC and Si-DLC films deposited on nitrile rubber

M. Lubwama, B. Corcoran, K.V. Rajani, C.S. Wong, J.B. Kirabira, A. Sebbit, K.A. McDonnell, D. Dowling, K. Sayers

PII: S0257-8972(13)00505-7
DOI: doi: 10.1016/j.surfcoat.2013.06.013
Reference: SCT 18594

To appear in: *Surface & Coatings Technology*

Received date: 16 November 2012
Accepted date: 4 June 2013

Please cite this article as: M. Lubwama, B. Corcoran, K.V. Rajani, C.S. Wong, J.B. Kirabira, A. Sebbit, K.A. McDonnell, D. Dowling, K. Sayers, Raman analysis of DLC and Si-DLC films deposited on nitrile rubber, *Surface & Coatings Technology* (2013), doi: 10.1016/j.surfcoat.2013.06.013

Raman analysis of DLC and Si-DLC films deposited on nitrile rubber

M. Lubwama [a,*], B. Corcoran[a], K.V. Rajani[b], C.S. Wong[b], J.B. Kirabira[c], A. Sebbit[c], K.A. McDonnell[d], D. Dowling[d], K. Sayers[e]

[a]School of Mechanical and Manufacturing Engineering, Dublin City University, Dublin 9, Ireland
[b]School of Electronic Engineering, Dublin City University, Dublin 9, Ireland
[c]Department of Mechanical Engineering, Makerere University, P.O. BOX 7062, Kampala, Uganda
[d]School of Mechanical and Materials Engineering, University College Dublin, Dublin 4, Ireland
[e]Department of Mechanical Engineering, Dundalk Institute of Technology, Dundalk, Ireland

.
*Corresponding author. Tel.: +353-89-954-2968; Fax: +353 -1-700-5345
E-mail address: michael.lubwama2@mail.dcu.ie (M. Lubwama)

Keywords: DLC; Si-DLC; G peak dispersion; Nitrile rubber; Raman spectroscopy; Tauc gap.

Abstract

In this study a hybrid diamond-like carbon (DLC) and silicon doped diamond-like carbon (Si-DLC), with and without Si-C interlayers, were deposited onto nitrile rubber substrates. The deposition was done in a closed field unbalanced magnetron sputtering ion plating (CFUBMSIP) rig in Ar/C_4H_{10} plasma. A combination of visible (488 nm) and ultra-violet (UV; 325 nm) Raman analysis was used to determine the G-peak dispersion of the films. Raman analysis was also used to estimate the hydrogen concentration and residual stress in the films. Calculated hydrogen values for all of the films were between 26 and 31%. The residual stress estimates of the films indicated that the inclusion of Si dopant and Si-C interlayers reduced compressive stress in these films. Raman analysis of the wear tracks indicated an increase in the G-peak position which could indicate that graphitization occurred during pin-on-disc experiments.

1. Introduction

Diamond-like Carbon (DLC) films have been studied extensively for over four decades since the pioneering work of Aisenberg and Chabot [1]. DLC is a metastable form of amorphous carbon containing a significant fraction of carbon (C) sp^3 hybridisations [2]. DLC films have also been defined as composites of nano-crystalline diamond and/or amorphous carbon with or without hydrogen. Hydrogen is required to passivize the dangling bonds of carbon [3].

Generally, the term "DLC" is commonly used to designate the hydrogenated form of diamond-like carbon (a-C:H), while the term "ta-C" (tetrahedral carbon) is used to designate non-hydrogenated carbon (a-C), containing high fractions of sp^3 hybridized carbon [2]. Amorphous carbons can be classified into four types including: polymer-like a-C:H (PLCH); diamond-like a-C:H (DLCH); hydrogenated tetrahedral amorphous carbon films (ta-C:H); and, graphite-like a-C:H (GLCH) [2,4].

Recently, the deposition and characterization of DLC and DLC related films onto rubber substrates has attracted significant interest due to possible applications onto piston seals and bearings in the automotive, aerospace and water supply industries [5-8]. These studies have shown improved tribological performance in terms of lower friction coefficients and wear rates for DLC and DLC based films deposited on rubber substrates in comparison to uncoated rubber [5-8]. The potential of smart detection of wear of DLC films has been enhanced by recent publications that show good piezo-resistive properties [9,10]. However, for DLC films deposited on rubber few studies have investigated the chemical and structural bonding of these films.

Takikawa *et al*. analysed DLC films deposited on ethylene propylene diene monomer (EPDM) rubber with a laser micro Raman spectrophotometer and found that for all of the films typical DLC spectra with a broadened hybrid spectra of the G-band (at approximately 1580 cm^{-1}) and D-band (at approximately 1380 cm^{-1}) were observed [11]. A weak shoulder at approximately 1150 – 1200 cm^{-1} appeared only for the film prepared under C_2H_2. Similar results were observed by Miyakawa *et al.* using a hybrid physical-chemical deposition technology [12].

Yoshida *et al*. used Raman spectroscopy analysis to identify DLC films deposited on silicone rubber [13]. A broad peak centred at 1530 cm^{-1} was measured for the film deposited on silicone rubber. A double Gaussian peak analysis was used to quantify the intensity ratio, I_D/I_G. It was found that the ratio of I_D/I_G for DLC deposited on Si wafer was higher than for DLC deposited on silicone rubber. Yoshida et al concluded that the sp^3 content in the films deposited on silicone rubber was therefore higher [13].

Martinez-Martinez *et al.* studied the chemical bonding of DLC films deposited on ACM rubber by means of Raman spectroscopy using a 532 nm excitation wavelength for DLC films prepared at different voltages (300, 400 and 600 V) [14]. G peak positions in the range 1528 – 1539 cm^{-1} and intensity ratios (I_D/I_G) in the range 0.4 – 0.5 were reported. The low I_D/I_G ratio and G position were attributed to high structural disorder of the carbon network. Martinez-Martinez et al. concluded that change in bias voltage did not have a significant influence on the sp^2 content, but rather on the structural and topological disorder [14].

Lubwama *et al.* used Raman spectroscopy to investigate the intensity ratio, I_D/I_G, for DLC and Si-DLC films with and without Si-C interlayers [5]. With the inclusion of the Si-C

interlayer the I_D/I_G ratio was observed to increase for both DLC and Si-DLC films with the highest intensity ratio of 1.2 recorded for Si-DLC film with Si-C interlayer. This increase in intensity ratio was attributed to an increase in sp^2 hybridized carbon in the films [5,6].

A review of the literature on Raman analysis of DLC films deposited on rubber has led to the following conclusions; Firstly, most of the Raman analysis was performed at visible excitation energies. Very few UV Raman spectroscopy analyses have been carried out for DLC and DLC based films deposited on rubber substrates [11,12,14]. UV Raman is particularly useful for hydrogenated amorphous carbons as it gives clear measurements in the D and G peaks spectral region even for highly hydrogenated samples, for which the visible Raman spectra are overshadowed by photoluminescence [4]. Multi-wavelength Raman spectra can be used to derive the structural properties of different types of amorphous carbons. Such a multi-wavelength analysis was recommended by Casiraghi et al to determine G-peak dispersion, Disp(G) [4]. Also, Raman spectroscopy analysis has been used to successfully determine the wear mechanisms involved during tribo-tests for DLC films sliding against metals by analysing the wear track before and after tribo-testing [15,16]. No evidence of such an analysis could be found in the literature for DLC films deposited on rubber substrates.

In this study, the Disp(G) was determined using a multi-wavelength Raman analysis. H content and residual stress estimates were calculated from visible Raman spectra (488 nm). The Raman analysis of the wear tracks was done by investigating the shifts in the G-peak position, the intensity ratio, I_D/I_G, and full width half maximum of G peak, FWHM(G), for the films deposited on nitrile rubber before and after pin-on-disc experiments.

2. Experimental

Acrylonitrile butadiene rubber (nitrile rubber) sheet of 3 mm thickness was used as the substrate in this study. Deposition of DLC and Si-DLC films with and without Si-C interlayers were carried out by a closed field unbalanced magnetron sputtering ion plating (CFUBMSIP) system in Ar/C_4H_{10} plasma (12 sccm/8sccm). A pulsed DC (p–DC) power unit (Advanced Energy) was used as substrate bias source, operating at frequency of 150 kHz with a pulse off time of 150 ns at a substrate voltage bias of –30 V. This bias voltage was maintained during the entire deposition process. Three pieces of nitrile rubber 100 mm by 100 mm by 3mm cut out from the same sheet were coated in each batch. Two opposite magnetrons were used as carbon targets and one magnetron was used as the Si target. The fourth magnetron in the system was not used during the deposition process. The samples were mounted on a holder in the centre of the system facing outwards towards the target. The sample rotation speed was 5 rpm. The NBR substrates were etched in Ar plasma for 10 min. at a bias of 200 V in order to clean the surface of contaminants and improve the adhesion of the carbonaceous layer. The total deposition time for DLC was 60 min. This process was repeated for all samples including for Si-DLC samples. In order to achieve the dopant of Si in Si-DLC, a current of 0.5 A was supplied to the Si target during the deposition. The Si-C interlayer was obtained by supplying a current of 1 A to the Si target and 1 A to the pure C target. The Si-C interlayer deposition time was 35 min. and the subsequent time for DLC deposition was 40 min. The elemental composition of Si (at. %) in the films determined by Energy Dispersive X-ray (EDX) is shown in Table 1. The thickness of the DLC and Si-DLC film deposited on the nitrile rubber was approximately 1.2 μm. With the Si-C interlayer included the thickness of the DLC and Si-DLC films was 500 nm and the Si-C interlayer was also 500 nm thick. Further details of the deposition set-up, deposition process, process design

and film properties including surface roughness, film thickness, have already been reported [5,6].

Raman spectra were acquired to investigate the chemical bonding of these films by using a LabRAM Horiba Jobin Yvon spectrometer equipped with a CCD detector using a UV laser at 325 nm for UV Raman spectra and an Ar laser at 488 nm for visible Raman spectra at 8 mW. All of the measurements were recorded for a spectral range of 500 to 3000 cm^{-1} for the same conditions (5 s of integration time and 5 accumulations) using a 100× magnification and a 200 µm pinhole. De Wolf showed that the penetration depth of the Raman spectra is inversely related to the absorption coefficient [17]. For all of these films the penetration depth was estimated as being below 500 nm for a wavelength of 488 nm (2.541 eV) for an absorption coefficient range between approximately 22000 and 30000 cm^{-1} (see Fig. 3b).

The combination of visible and UV Raman spectra can be used to define Disp(G). Disp(G) is defined as the rate of change of G peak position with excitation wavelength [4,18]. Disp(G) of DLC and Si-DLC films has been studied by means of a multi-wavelength Raman analysis using a 325 nm (UV) and 488 nm (visible) excitation wavelengths. Disp(G) of the films was determined from equation (1) [18].

$$Disp(G) = \left| \frac{Pos(G)@\lambda_2 - Pos(G)@\lambda_1}{\lambda_2 - \lambda_1} \right| \qquad (1)$$

where Pos(G) @ $\lambda_{1,2}$ is the G-peak position at 488 and 325 nm respectively.

The photoluminescence (PL) background of DLC films has been related to bonded hydrogen in the films [3,4]. The PL background was measured from 488 nm Raman spectra. This is defined as the ratio between the slope of the Raman spectra (m) between 800 and 1900 cm^{-1}

as depicted in Fig. 1. Fig. 1 also shows a typical double Gaussian fit to determine Raman parameters. The bonded hydrogen in the DLC and Si-DLC films was estimated using equation (2) valid for H > 20 at. % [4].

$$H[at.\%] = 21.7 + 16.6\left\{log\left(\frac{m}{I_G}\right)[\mu m]\right\} \qquad (2)$$

where m is the slope (dy/dx) of the fitted linear photoluminescence (PL) background from G peak position 800 cm^{-1} to 1900 cm^{-1}, and I_G is the intensity of the G peak. I_G was calculated after background subtraction.

The Tauc gap, E_T, was derived by UV-visible spectrophotometry (Perkin Elmer Lambda 40 UV-Vis spectrometer) for DLC and Si-DLC films with and without Si-C interlayer deposited on standard glass microscope slides (manufactured to BS 7011). The deposition was done under the same processing conditions and time as the films deposited on nitrile rubber. The bonded hydrogen (H > 20 at. %) for these films was estimated using equation (3) that relates Tauc gap (E_T) and hydrogen content [4].

$$H[at.\%] = \frac{E_T[eV]+0.9}{0.09} \qquad (3)$$

For an amorphous material the Tauc gap can be estimated using the relation between absorption coefficients (α) and incident photon energy (hν) as shown in equation (4) (A is a constant and E_T is the Tauc gap of the material) [19]. Extrapolating the linear portion of the $(\alpha h\nu)^{1/2}$ vs. hν plot to the hν axis at α = 0, the Tauc gap can easily be determined. The E_{04} gap is determined from a plot of the absorption coefficient, α, vs. photon energy, indicating the typical Urbach-like tail, at the point where the absorption coefficient $\alpha = 10^4$ cm^{-1} [20].

$$\alpha h\upsilon = A(h\upsilon - E_T) \qquad (4)$$

Equation (5) relates the scale of the Raman shift is to the residual stress σ as follows [21]:

$$\sigma = 2G\left\{\frac{1+\upsilon}{1-\upsilon}\right\}\left\{\frac{\Delta w}{w_0}\right\} \qquad (5)$$

where Δw is the shift in Raman wavenumber of the G peak, w_o is the Raman wavenumber of reference, G is the shear modulus (G = 70 GPa [22]) and ν is Poisson's ratio (ν = 0.3 [22]).

Visible Raman spectra (488 nm) of the wear tracks were obtained before and after tribo-tests. The tribo-tests were carried out using a pin-on-disc (POD 2) tribometer. The counterpart was a standard Ø5 mm commercial stainless steel (DIN 5401) ball. The sliding speed was maintained at a linear speed of 10 cm/s at correlative test track diameters of 6 mm. Tribo-tests were carried out for normal load of 1 N and 5 N under both dry sliding and wet sliding conditions. Wet sliding was achieved by attaching a pipette filled with water adjacent to the pin so that its position ensures that a continuous flow of water was dispensed. Prior to commencement of wet sliding tests, water was dispensed onto the coated samples so that an initial boundary lubrication contact was achieved [5]. The wear tracks were characterised using a digital microscope (Keyence 3D VHX-2000).

3. Results and discussion

3.1. G-peak dispersion (Disp(G))

Fig. 2 shows typical Raman spectra at excitation wavelength of 325nm and 488 nm for DLC and Si-DLC films deposited on nitrile rubber. The PL background features prominently for visible Raman spectra obtained at 488 nm excitation wavelength. The photoluminescence

background is related to the bonded hydrogen in the film [4,12,23]. The main effect of hydrogen in hydrogenated DLC films is to modify the C-C network [3,4]. The Raman spectra are not identical in Fig.2, despite the deposition process being reproducible due to influence of the Si-C interlayer in Raman spectra shown in Fig. 2c and 2d. The estimated penetration depth of Raman spectra in this study was below 500 nm, but when the top film DLC and Si-DLC film is being deposited on the Si-C interlayer some ion exchange during magnetron sputtering deposition should be expected. For UV Raman spectra, the T peak at 1150 cm^{-1} is observed. The T peak is due to the C sp^3 – C sp^3 vibrational modes [24]. Quantitative determination of sp^3 hybridisation content using the T peak has only been shown for hydrogen free DLC films. In hydrogenated DLC films the presence of the D peak limits the determination of sp^3 content [25].

From equation (1) and Fig. 2, Disp(G) for DLC, Si-DLC, DLC with Si-C interlayer and Si-DLC with Si-C interlayer was 0.11, 0.10, 0.15 and 0.09, respectively. These low values for Disp(G) can be attributed to the deposition technology used in this study. The combination of a CFUBMSIP system and reactive magnetron sputtering in an Ar/C_4H_{10} plasma may explain these results. This deposition method allows DLC to be deposited onto nitrile rubber resulting in G peaks at approximately 1580 cm^{-1}, which is close to the graphite vibrational density of states [23]. Cui *et al.* also reported Disp(G) values below 0.20 for hydrogenated DLC films deposited on Si wafers using an arc ion plating system [18]. Casiraghi *et al.* reported Disp(G) results of 0.16 for DLCH films deposited by magnetron sputtering and 0.12 for GLCH films deposited by plasma enhanced chemical vapour deposition [4]. These values for Disp(G) are lower than Disp(G) results reported for ta-C:H and PLCH, which have Disp(G) values of 0.25 to 0.30 and 0.30 to 0.40, respectively [4]. Also in previous studies the Disp(G) was

determined using positions of the G peak at 514 nm and 244 nm excitation wavelengths [4,18].

For UV Raman excitation the G peak position decreases with increasing sp^2 clustering [4]. Therefore, if two samples have similar G peak positions in visible Raman but different ones in UV Raman, the sample with lower G peak position in UV has higher sp^2 clustering [4]. Therefore, DLC film with Si-C interlayer has more sp^2 clustering.

3.2. Hydrogen estimation

The presence of a PL background for the visible spectra (488 nm) for DLC and Si-DLC films deposited on nitrile rubber is an indicator of bonded hydrogen in the films [3,4,23]. From equation (2) and Fig. 1, the bonded hydrogen content in the films was determined. Calculated hydrogen values for all of the films were between 26 and 31%. This implies that the films deposited on nitrile rubber can be classed as diamond-like a-C:H (DLCH) which has 20 – 40 at. % hydrogen [2].

The presence of hydrogen in hydrogenated DLC films is to modify the C-C network [4,23]. The introduction of hydrogen into an amorphous carbon links the amount and configuration of the C sp^2 phase with the overall C sp^3 hybridisation [4]. However, for increments of hydrogen over 25% at., the overall sp^3 hybridisation can still increase, but not the C sp^3 – C sp^3 bonding [4].

The Tauc gap was observed to decrease slightly for DLC from 1.63 eV to 1.57 eV for DLC with Si-C interlayer. For Si-DLC the Tauc gas was 1.45 eV, and this increased to 1.52 for Si-

DLC with Si-C interlayer. The E_{04} gaps for the films was 2.06 eV for DLC, 1.99 eV for Si-DLC, 2.12 eV for DLC with Si-C interlayer, and 2.02 eV for Si-DLC with Si-C interlayer. Casiraghi *et al.* reported similar results [4]. These results were consistently reproduced on measurements made on a series of different samples deposited under the same conditions.

This result further characterises the films deposited as diamond-like a-C:H (DLCH) which have an optical gap between 1 and 2 eV [2]. The Tauc gap is mainly determined by the status of C sp^2 hybridization clusters imbedded in the amorphous carbon medium [26]. The increase in the Tauc gap can be explained by the cluster model theory proposed by Robertson [27]. The increase in the Tauc gap for the Si-DLC film with Si-C interlayer compared with the Si-DLC film implies that the sp^3 content increases which promotes the disordering in the films and lowers the sp^2 cluster size [19]. The decrease in Tauc gap for the DLC film with Si-C interlayer compared to the DLC film may be due an increase in the size of C sp^2 hybridized graphitic clusters in these films [28,29]. This result is consistent with the discussion above on Disp(G) where the DLC with Si-C interlayer film was noted to have more sp^2 clustering.

Using the measured values of the Tauc gap and equation (3) the bonded hydrogen in the films was estimated. The bonded hydrogen (at. %) was determined as 28.1% for DLC, 26.1% for Si-DLC, 27.4% for DLC with Si-C interlayer, and 26.9% for Si-DLC with Si-C interlayer. These results are shown in Fig. 4. For hydrogen estimation using the PL background method, the results indicate that the hydrogen content in the samples is independent of doping with Si and the Si-C interlayer. Comparison of hydrogen content is particularly good using both methods for DLC and DLC with Si-C interlayer films. This implies that bonded hydrogen in the films is determined more by the reactive mechanisms that proceed between Ar gas and C_4H_{10} gas during the deposition stage of these films.

3.3. Residual stress

The G peak position for Si-DLC, DLC with Si-C interlayer, and the Si-DLC with Si-C interlayer was 1584 cm^{-1}, while that for DLC film was 1580 cm^{-1}, for visible Raman spectra at 488 nm. Selecting the G peak position of the DLC film as the reference Raman wavelength in equation (5) the relative residual stress can be calculated for Si-DLC, DLC with Si-C, and Si-DLC with Si-C, deposited on nitrile rubber for the deposition conditions used in this study.

Relative residual stress of values 0.66 GPa for Si-DLC, DLC film with Si-C interlayer and Si-DLC film with Si-C interlayer compared to DLC film are calculated. These G peak positions shift upwards in all cases. This is indicative of lower amounts of internal compressive stress compared to DLC film [21]. In this work we took the DLC film as a reference, which may not indicate sufficiently the extent of the lower amounts of residual stress in the films as they were all deposited using the same deposition technology and the variation of 4 cm^{-1} may be within measurement error; however, once comparisons are made to results reported elsewhere for DLC films deposited rubber where G peak values of between 1528 -1539 cm^{-1} [14], then the magnitude of internal compressive stress reduction in the films in this study becomes clear.

The residual stress arises as a result of the correlation between the interatomic force constant and interatomic separation. The interatomic force constant is associated with the atomic vibrational frequency. If the tensile load on the material increases, bond lengths increase, force constants decrease, and vibrational frequencies decrease. On the other hand, if a material is subjected to mechanical compression, bond lengths decrease, force constants

increase, and vibrational frequencies increase [21]. However, silicon cannot significantly contribute to internal stress reduction in diamond-like carbon–silicon composite films, since silicon atoms tetrahedrally bond to carbon and other silicon atoms [21].

3.4. Raman analysis of wear track

Generally, the visible Raman spectra (488 nm) for all of the wear tracks (see Fig. 5 and Fig. 6) were characterised by a broad C-H stretching band around 2800 – 2900 cm^{-1}, further supporting the classification of these films as hydrogenated amorphous carbons [12]. Raman curves for nitrile rubber and Si-C interlayer passed the same wear test as the coatings prior to measurement. For dry sliding under normal load of 1 N and 5 N, the increased PL background for the Si-DLC, DLC with Si-C and Si-DLC with Si-C interlayer films are increased compared to DLC film is attributed to Si (at. %) present in these films [19]. After wet sliding the PL background increases for all of the films under normal load of 1 N and 5 N. The increase in PL background is attributed most probably to a tribo-chemical reaction between the films and the water to form various hydroxyl groups [30].

For both dry and wet sliding under normal load of 1 N no penetration of all of the films was observed with a corresponding increase in the G-peak value for all of the films after tribo-testing (see Table 1). These results indicate a progressive transformation of sp^3 structure towards a more graphite-like sp^2 structure at the wear track [15,16,31]. The G peak shift upwards is also attributed to a progressive reduction of defects (bond angle and bond-bending disorder) in the sp^2 amorphous carbon network. These changes can be explained by an increment in number, size, and order of sp^2 aromatic clusters from an initial amorphous sp^2-carbon network [32].

For dry sliding under normal load of 5 N, there was penetration of all of the films after tribo-testing, except for DLC with Si-C interlayer. From a comparison of the Raman spectra of the Si-C interlayer and rubber substrate with the Raman spectra of the DLC and Si-DLC films with and without Si-C interlayer after tribological tests, it is clear that the nitrile rubber substrate and Si-C interlayer modify the Raman response of the films (see Fig. 6a). The performance of the DLC with Si-C interlayer film is attributed to increase in the size of C sp^2 hybridized graphitic clusters in these films. For wet sliding under normal load of 5 N, there was no penetration of all of the films after tribo-testing. This is due to the water molecules saturating on the film surfaces and decreasing the amount of dangling bonds between the films and counterpart [33].

Fig. 7 shows intensity ratio, I_D/I_G, and the full width half maximum of the G peak, FWHM(G), for the wear tracks of the films deposited on nitrile rubber. Data for dry sliding under normal load of 5 N are not reported as complete film penetration was observed for these films except for DLC with Si-C interlayer. For the DLC and DLC film with Si-C interlayer I_D/I_G ratio are higher than before wear testing which generally implies that the sp^2 content in these films is increasing [23]. The FWHM(G) for all of the films is below the values before tribo-testing which suggests that the graphitic clusters within the films were unstrained [34]. FWHM(G) is mainly sensitive to structural disorder, which arises from bond angle and bond length distortions. Therefore, the low values of FWHM(G) are attributed to reduction of defects in the sp^2 amorphous carbon networks indicating a more graphitic organization and a decrease of C sp^3 – C sp^3 bonding percentage [34,35].

4. Conclusion

In this study a hybrid diamond-like carbon (DLC) and silicon doped diamond-like carbon (Si-DLC), with and without Si-C interlayers, were deposited onto nitrile rubber substrates. The deposition was done in a closed field unbalanced magnetron sputtering ion plating (CFUBMSIP) rig in Ar/C_4H_{10} plasma. A combination of the visible (488 nm) and ultra-violet (UV) Raman analysis (325 nm) was used to determine Disp(G) for the films. Disp(G) analysis showed that DLC with Si-C interlayer film has more sp^2 clustering. For hydrogen estimation using the PL background method, the results indicate that the hydrogen content in the samples is independent of doping with Si and the Si-C interlayer. Calculated hydrogen values for all of the films were between 26 and 31%. The residual stress estimates of the films indicated that the inclusion of Si dopant and Si-C interlayers reduced compressive stress in these films. For dry sliding the increased PL background for the Si-DLC, DLC with Si-C and Si-DLC with Si-C interlayer films are attributed to Si (at. %) present in these films. The increase in PL background for wet sliding is attributed to tribo-chemical reactions between the films and the water to form various hydroxyl groups. For both dry and wet sliding under normal load of 1 N no penetration of all of the films was observed with a corresponding increase in the G-peak value. This indicated a progressive transformation towards a more graphite-like sp^2 structure on the wear track. For dry sliding under normal load of 5 N, there was penetration of all of the films after tribo-testing, except for DLC with Si-C interlayer. The performance of the DLC with Si-C interlayer film is attributed to increase in the size of C sp^2 hybridized graphitic clusters. For wet sliding under normal load of 5 N, there was no penetration of all of the films after tribo-testing. This is due to the water molecules saturating on the film surfaces and decreasing the amount of dangling bonds between the films and counterpart.

Acknowledgements

The authors would like to acknowledge the financial support provided by the Water is Life project under Irish Aid and Higher Education Authority partnership of The Republic of Ireland for the financial support to carry out the research.

References

[1] S. Aisenberg and R. Chabot, J. Appl. Phys. 42 (1971) 2953.

[2] J. Robertson, Materials Science and Engineering: R 37 (2002) 129.

[3] A. Singha, A. Ghosh, A. Roy, N.R. Ray, J. Appl. Phys. 100 (2006) 044910.

[4] C. Casiraghi, A.C. Ferrari, J. Robertson, Phys. Rev. B 72 (2005) 085401.

[5] M. Lubwama, K.A. McDonnell, J.B. Kirabira, A. Sebbit, K. Sayers, D. Dowling, B. Corcoran, Surf. Coat. Technol. 206 (2012) 4585.

[6] M. Lubwama, B. Corcoran, K. Sayers, J.B. Kirabira, A. Sebbit, K.A. McDonnell, D. Dowling, Surf. Coat. Technol. 206 (2012) 4881.

[7] T. Nakahigashi, Y. Tanaka, K. Miyake, H. Oohara, Tribology International 37 (2004) 907.

[8] Y.T. Pei, X.L. Bui, J.T.M. De Hosson, Thin Sol. Films 518 (2010) S42.

[9] E. Peiner, A. Tibrewala, R. Bandorf, H. Luthje, L. Doering, W. Limmer, J. Micromech. Microeng. 17 (2007) S83.

[10] S. Meskinis, A. Vasiliauskas, K. Slapikas, R. Gudaitis, S. Tamulevicius, G. Niaura, Surf. Coat. Technol. 211 (2012) 172.

[11] H. Takikawa, N. Miyakawa, S. Minamisawa, T. Sakakibara, Thin Solid Films 457 (2004) 143.

[12] N. Miyakawa, S. Minamisawa, H. Takikawa, T. Sakakibara, Vacuum 73 (2004) 611.

[13] S. Yoshida, M. Okoshi, N. Inoue, J. Phys. : Conf. Ser. 59 (2007) 368.

[14] D. Martinez-Matrinez, M. Schenkel, Y.T. Pei, J.C. Sanchez-Lopez, J.T.M. De Hosson, Surf. Coat. Technol. 205 (2011) S75.

[15] Z.F. Zhou, K.Y. Li, I. Bello, C.S. Lee, S.T. Lee, Wear 258 (2005) 1589.

[16] W.S. Choi, M. Park, B. Hong, Thin Sol. Films 515 (2007) 7560.

[17] I. De Wolf, Semicond. Sci. Technol 11 (1996) 139.

[18] W.G. Cui, Q.B. Lai, L. Zhang, F.M. Wang, Surf. Coat. Technol. 205 (2010) 1995.

[19] S.F. Ahmed, D. Banerjee, M.K. Mitra, K.K. Chattopadhyay, J. Lumin. 131 (2011) 2352.

[20] K.B.K. Teo, A.C. Ferrari, G. Fanchini, S.E. Rodil, J. Yuan, J.T.H. Tsai, E. Laurenti, A. Tagliaferro, J. Robertson, W.I. Milne, Diamond Relat. Mater. 11 (2002) 1086.

[21] R.J. Narayan, Appl. Surf. Sci 245 (2005) 420.

[22] K. Nakamatsu, M. Nagase, J. Igaki, H. Namatsu, S. Matsui, J. Vac. Sci. Technol. B 23 (2005) 2801.

[23] A.C. Ferrari and J. Robertson, Phys. Rev. B 61 (2000) 14095.

[24] S. Piscanec, F. Mauri, A.C. Ferrari, M. Lazzeri, J. Robertson, Diamond & Rel. Mater. 14 (2005) 1078.

[25] K.W.R. Gilkes, S. Prawer, K.W. Nugent, J. Robertson, H.S. Sands, Y. Lifshitz, X. Shi, J. Appl. Phys. 87 (2000) 7283.

[26] J. Robertson, Surf. Coat. Technol. 50 (1992) 185.

[27] J. Robertson, Phil. Mag. Lett. 57 (1988) 143.

[28] J. Robertson and E. O'Reilly, Phys. Rev. B 35 (1987) 2946.

[29] S.R.P. Silva, J. Robertson, Rusli., G.A.J. Amaratunga, J. Schwan, Philos. Mag. B 74 (1996) 369.

[30] X. Wu, M. Suzuki, T. Ohana, A. Tanaka, Diamond Relat. Mater. 17 (2008) 7.

[31] Y. Liu, A. Erdemir, E.I. Meletis, Surf. Coat. Technol. 86-87 (1996) 564.

[32] J.C. Sanchez-Lopez, A. Erdemir, C. Donnet, T.C. Rojas, Surf. Coat. Technol. 163-164 (2003) 444.

[33] Y. Ozmen, A. Tanaka, T. Sumiya, Surf. Coat. Technol. 133-134 (2000) 455.

[34] R. Paul, S.N. Das, S. Dalui, R.N. Gayen, R.K. Roy, R. Bhar, A.K. Pal, J. Phys. D. Appl. Phys. 41 (2008) 055309.

[35] C. Jaoul, O. Jarry, P. Tristant, T. Merle-Mejan, M. Colas, C. Dublanche-Tixier, J.-. Jacquet, Thin Sol. Films 518 (2009) 1475.

List of Figures

Table 1
Summary of results for G peak position, ID/IG ratio, FWHM(G) for before and after tribology testing. Tauc gap, H and Si for the films are also shown.

		DLC	Si-DLC	DLC with Si-C Interlayer	Si-DLC with Si-C Interlayer
G-peak position [cm^{-1}]	Before	1580	1584	1584	1584
	Dry sliding (1 N)	1584	1586	1587	1587
	Wet sliding (1 N)	1591	1586	1587	1587
	Wet sliding (5 N)	1586	1586	1581	1581
I_D/I_G	Before	0.7±0.0	1.0±0.1	1.1±0.2	1.2±0.2
	Dry sliding (1 N)	1.1±0.1	0.9±0.2	1.3±0.1	1.2±0.1
	Wet sliding (1 N)	1.6±0.1	1.0±0.0	1.2±0.1	1.7±0.1
	Wet sliding (5 N)	0.9±0.1	1.1±0.1	1.2±0.1	1.2±0.1
FWHM(G) [cm^{-1}]	Before	86.9±13.8	89.1±27.7	96.5±9.4	94.1±20.1
	Dry sliding (1 N)	72.1±2.8	71.3±4.7	63.5±3.0	69.8±5.3
	Wet sliding (1 N)	60.1±3.5	68.8±5.2	70.1±4.2	65.1±6.5
	Wet sliding (5 N)	72.1±2.8	69.4±4.9	77.3±3.5	76.1±5.7
Tauc gap (E_T) [eV]		1.63	1.45	1.57	1.52
E_{04} gap [eV]		2.06	1.99	2.12	2.02
Disp(G) [cm^{-1}/nm]		0.11	0.10	0.15	0.09
Residual stress [GPa]		-	0.66	0.66	0.66
H [at. %] (PL method)		27.8±1.4	28.6±1.4	27.7±1.4	29.0±1.4
H [at. %] (Tauc gap method)		28.1±0.2	26.1±0.3	27.4±0.2	26.9±0.3
Si [at. %]		0.2±0.1	2.6±0.5	5.2±0.3	5.5±1.4

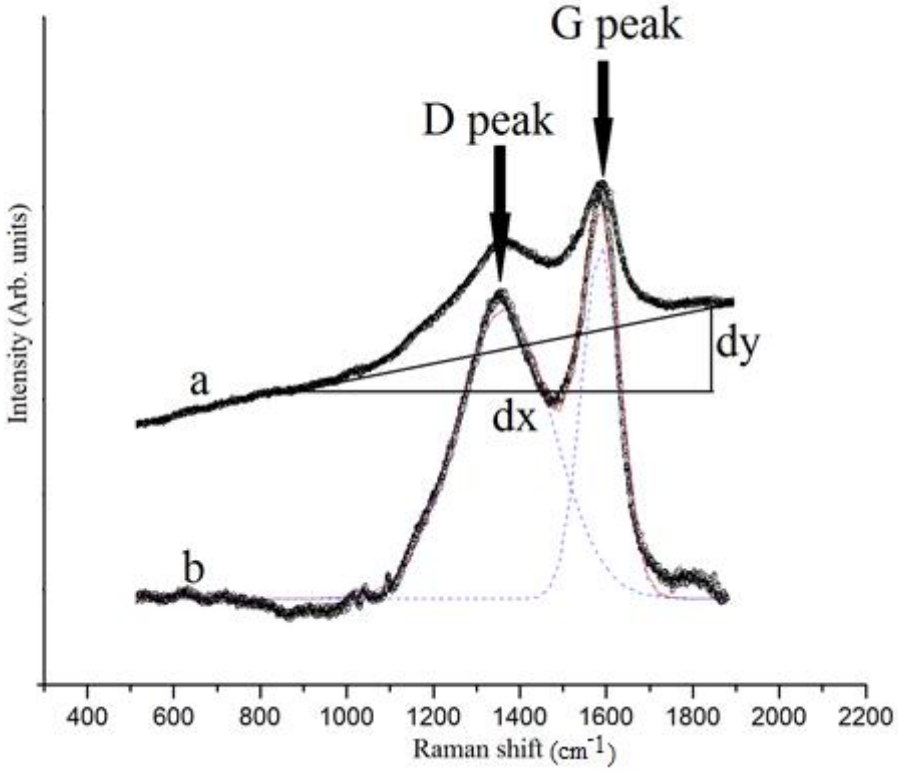

Fig. 1. Schematic representation for hydrogen estimation in the films (a); and a typical Gaussian fit to determine the Raman parameter. The hollow circles are experimental data points. The deconvoluted components are shown by dashed lines. The resultant fitted curve is shown by the solid line (b).

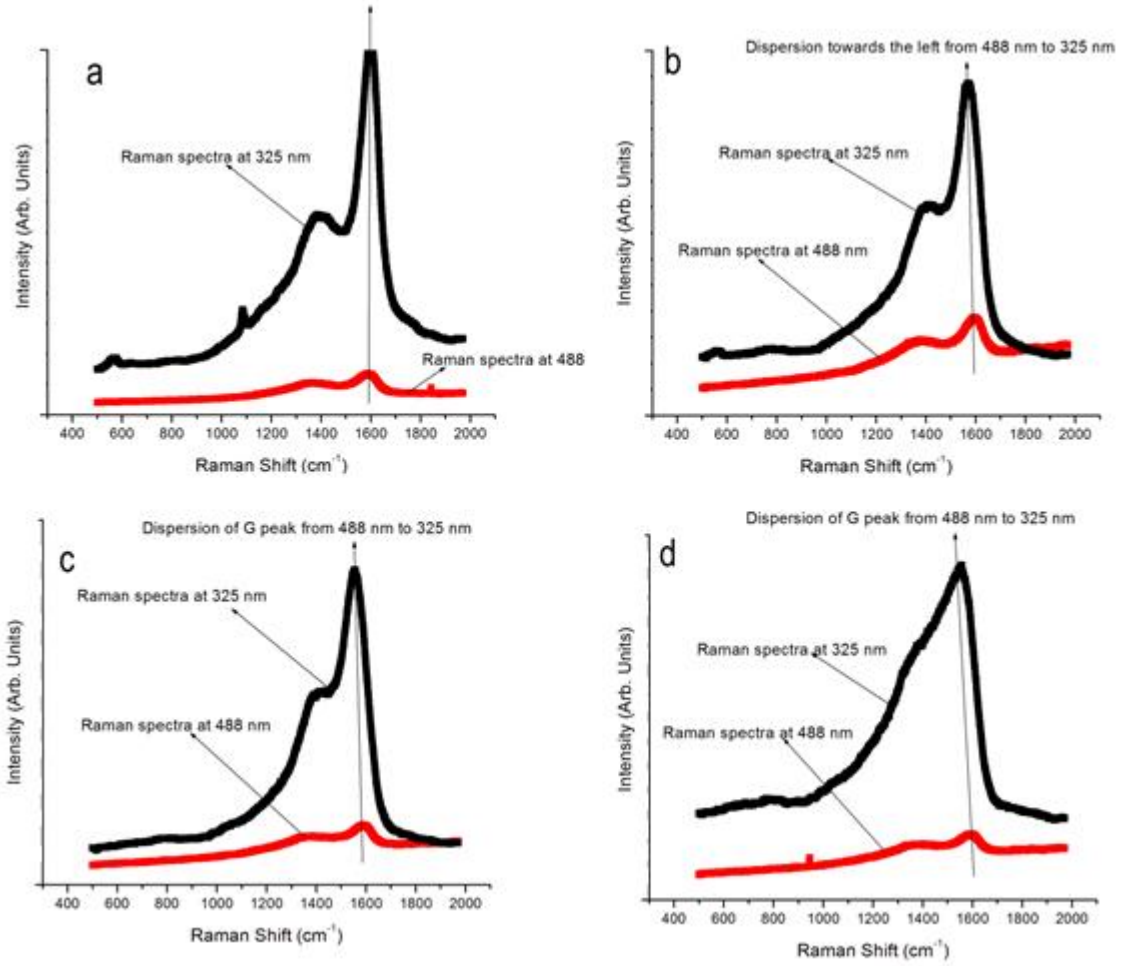

Fig. 2. Disp(G) from 488 nm to 325 nm for: a) DLC; b) Si-DLC; c) DLC with Si-C; d) Si-DLC with Si-C films deposited on nitrile rubber

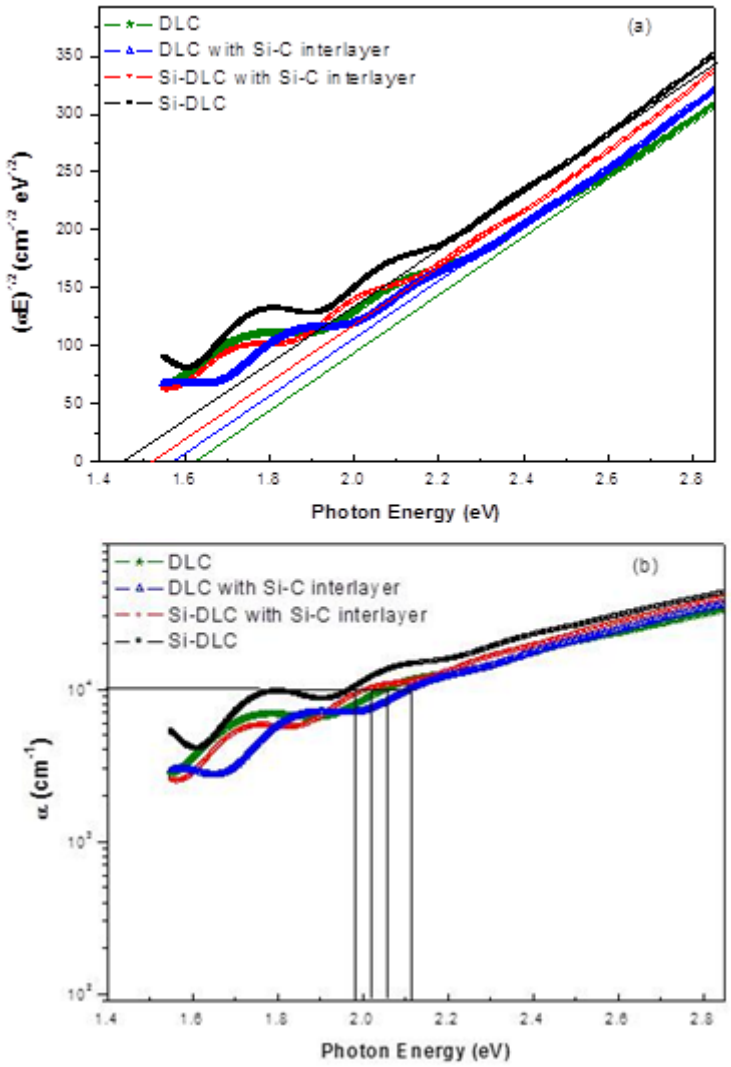

Fig. 3. Tauc plot for films derived from UV-Vis measurements (a) and, absorption coefficient, α, vs. photon energy (b).

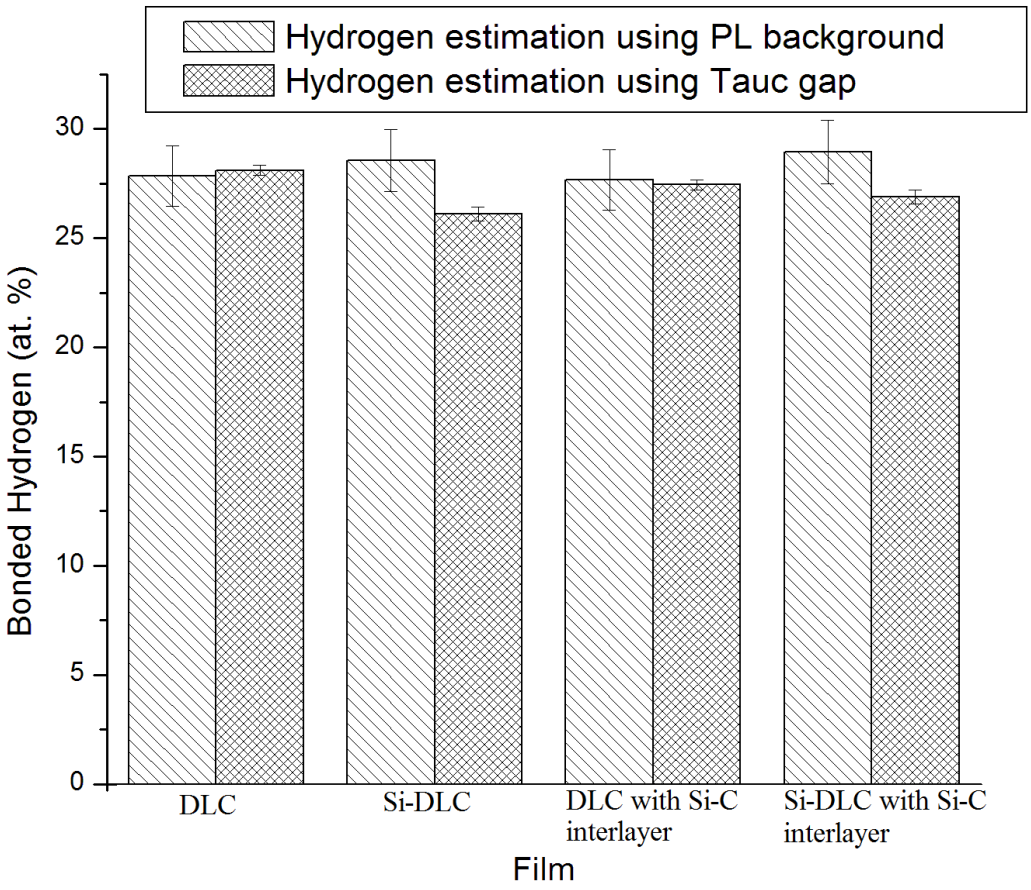

Fig. 4. Bonded hydrogen estimation using PL background and Tauc gap

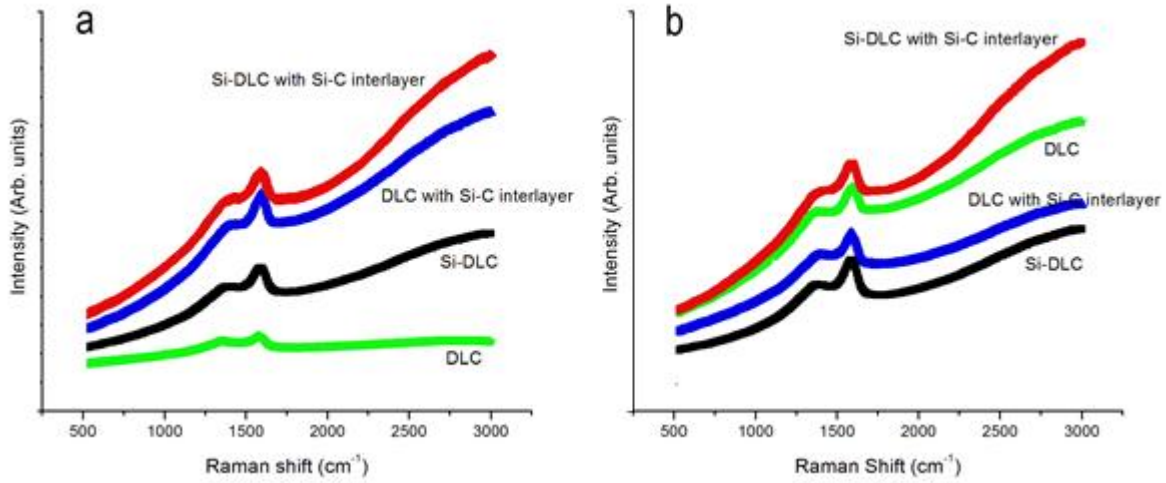

Fig. 5. Raman spectra (488 nm) of the wear tracks after pin-on-disc tests under normal load of 1 N under: a) dry sliding, and, b) wet sliding

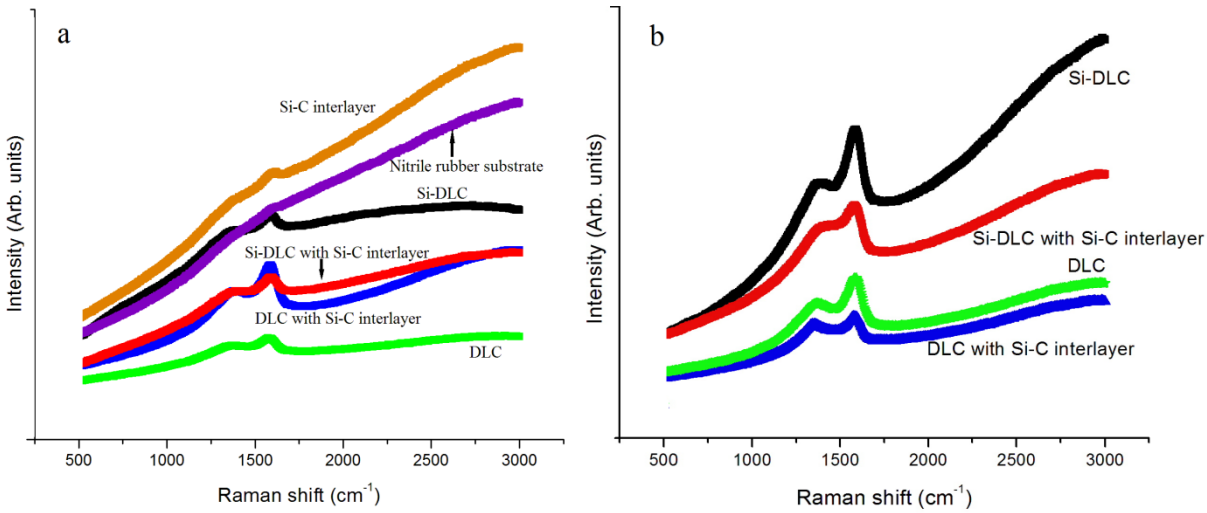

Fig. 6. Raman spectra (488 nm) of wear tracks after pin-on-disc tribo tests under a normal load of 5 N: a) dry sliding, and, b) wet sliding

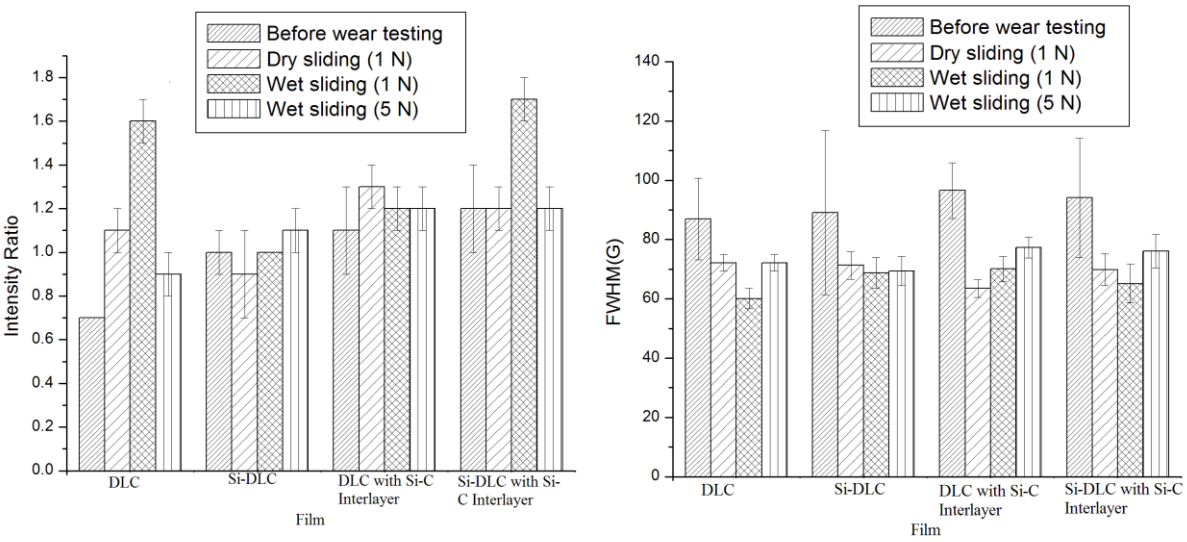

Fig. 7. Raman parameters for the wear tracks: a) Intensity ratio, I_D/I_G, and, b) full width half maximum of the G peak, FWHM(G)

Highlights

- DLC and Si-DLC films were deposited onto nitrile rubber
- G-peak dispersion was determined using multi-wavelength Raman spectroscopy
- DLC film with Si-C interlayer has more sp^2 clustering
- Calculated hydrogen values for all of the films were between 26 and 31%
- Graphitization processes occurred during pin-on-disc experiments